Supplementary Information

Supplementary Figures (1-7) & legends

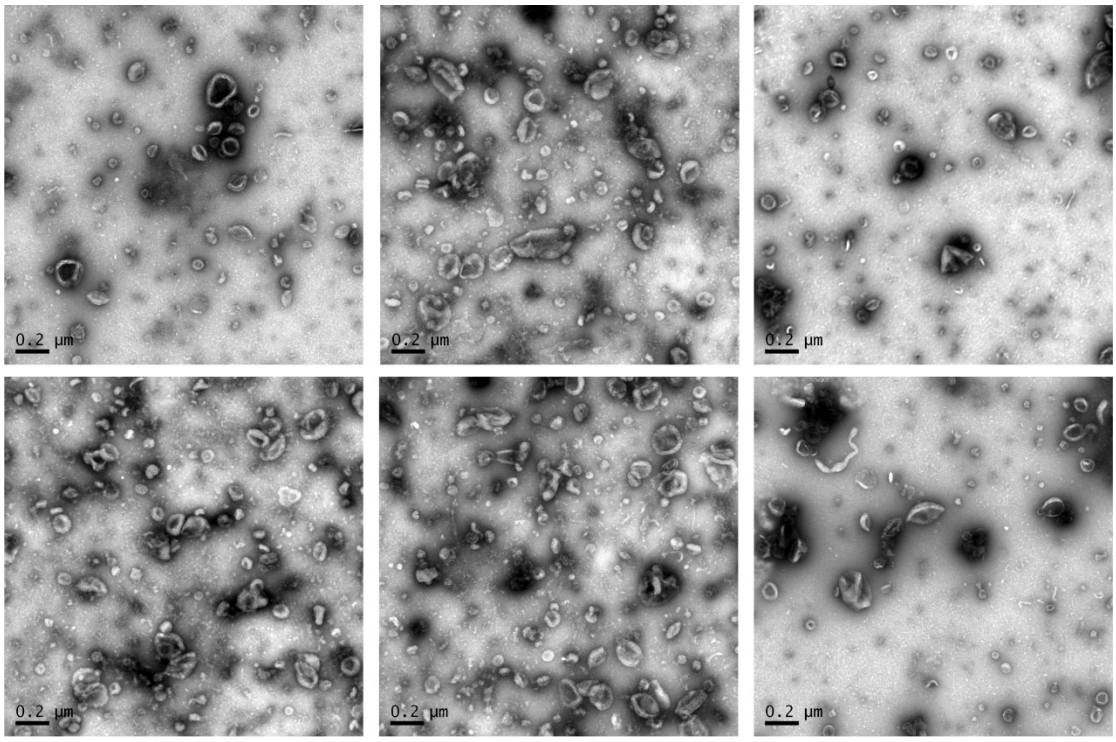

Supplementary Fig. 1 Lower-magnification TEM images of MVs. TEM images of purified MVs from GCs. Source data are provided as a Source Data file.

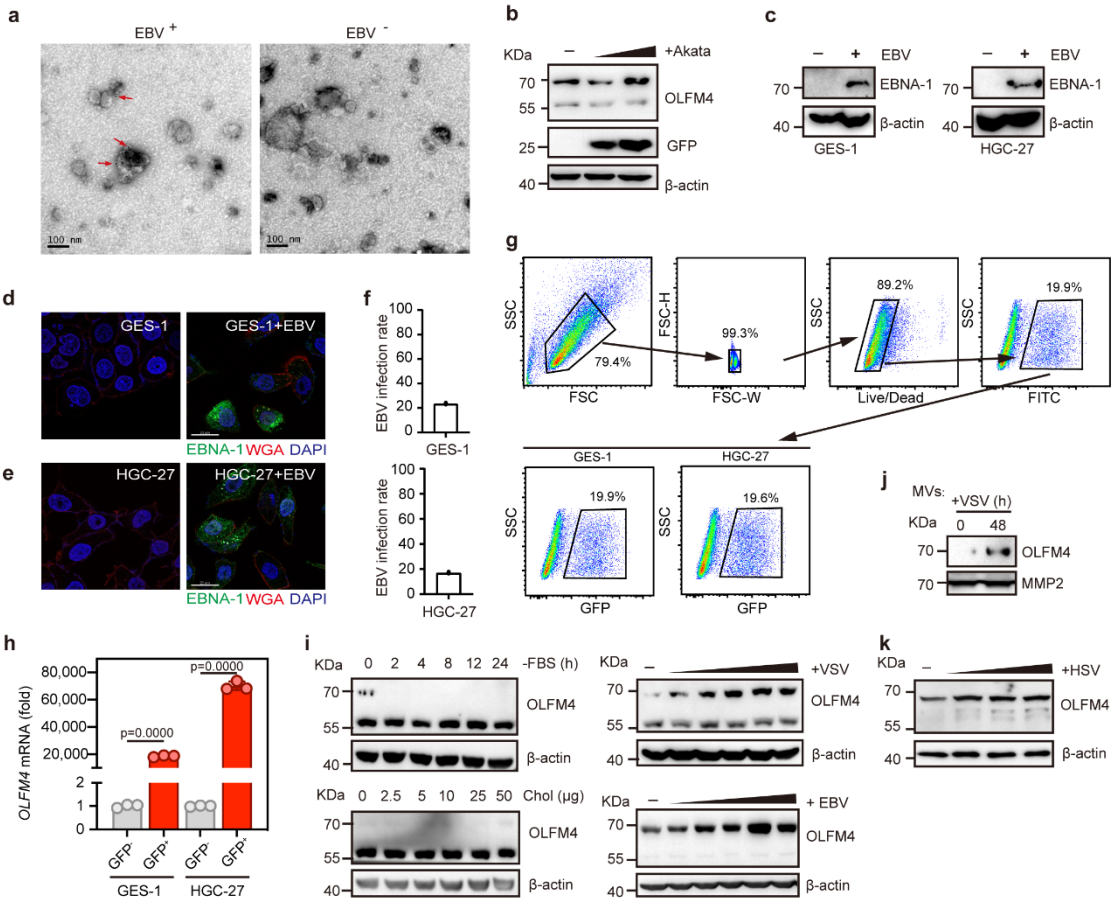

Supplementary Fig. 2 OLFM4 was induced by virus infection. a Immunogold electron microscopic labeling of MVs with antibodies specific to OLFM4. MVs are purified from EBV-positive or EBV-negative GC tissues. Red arrows indicate anti-OLFM4 immunogold particles. **b** Immunoblotting showing OLFM4 expression in EBV-infected AGS cells EBV by Akata cells. The EBV-positive Akata cells containing a GFP tag in the viral genome of EBV were co-cultured with AGS cells for 24 h. The dose gradient: 1×10^5, 1×10^6 Akata cells. **c** Immunoblotting showing the EBNA-1 expression in EBV infected GES-1 or HGC-27 cells. **d** Immunofluorescent images showing the infection rate of EBV in GES-1 cells. Scale bars, 20 μm. **e** Immunofluorescent images showing the infection rate of EBV in GES-1 cells. Scale bars, 20 μm. **f** Quantification for the infection rate of EBV in GES-1 and HGC-27 respectively. **g** FCS showing the proportion of GFP-positive cells in GES-1 and HGC-27 cells. **h** QPCR analysis of OLFM4 in EBV-infected GES-1 and HGC-27 cells (n=3 biological replicates/group). Data are presented as mean ± s.d., analyzed for significant differences

by performing two-tailed, one-way ANOVA with Dunnett's post hoc analysis. **i** Immunoblotting showing the intracellular OLFM4 in AGS cells with or without FBS for the indicate time, or treated with cholesterol (0, 2.5, 5, 10, 25, 50 μg/ml), VSV (0, 0.5, 1, 2.5, 5, 10 MOI) or EBV (0, 0.5, 1, 2 .5, 5, 10 MOI) for 24 h. Vesicular stomatitis virus (VSV) was produced from Vero cells. **j** Immunoblotting showing the expression of OLFM4 in VSV-infected AGS cells. Each lane was loaded with 2×10^8 MV particles. **k** Immunoblotting showing the expression of OLFM4 in HGC-27 cells infected by 0, 0.1, 1, 10 MOI HSV-1 (KOS strain) for 48 h. All lanes were loaded with 50 μg of total protein (b,f). Representative of 2 independent experiments (a-j). Source data are provided as a Source Data file.

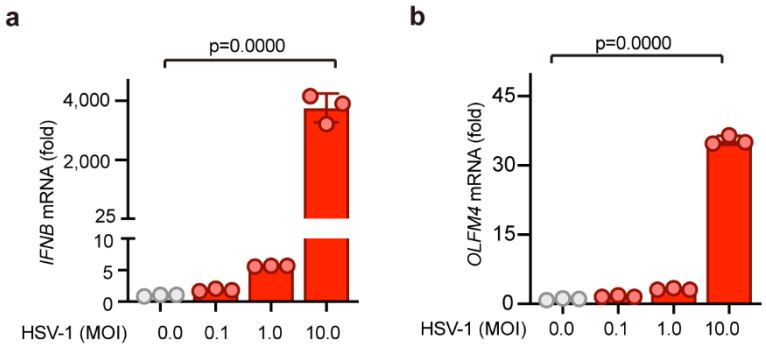

Supplementary Fig. 3 HSV-1 treatment induces OLFM4 upregulation. a mRNA levels of IFNB in HGC-27 cells after infection with HSV-1 for 48 h (n=3 biological replicates/group). **b** mRNA levels of OLFM4 in HSV-infected cells (n=3 biological replicates/group). Data are presented as mean ± s.d., analyzed for significant differences by performing two-tailed one-way ANOVA with Dunnett's post hoc analysis (a,b). Source data are provided as a Source Data file.

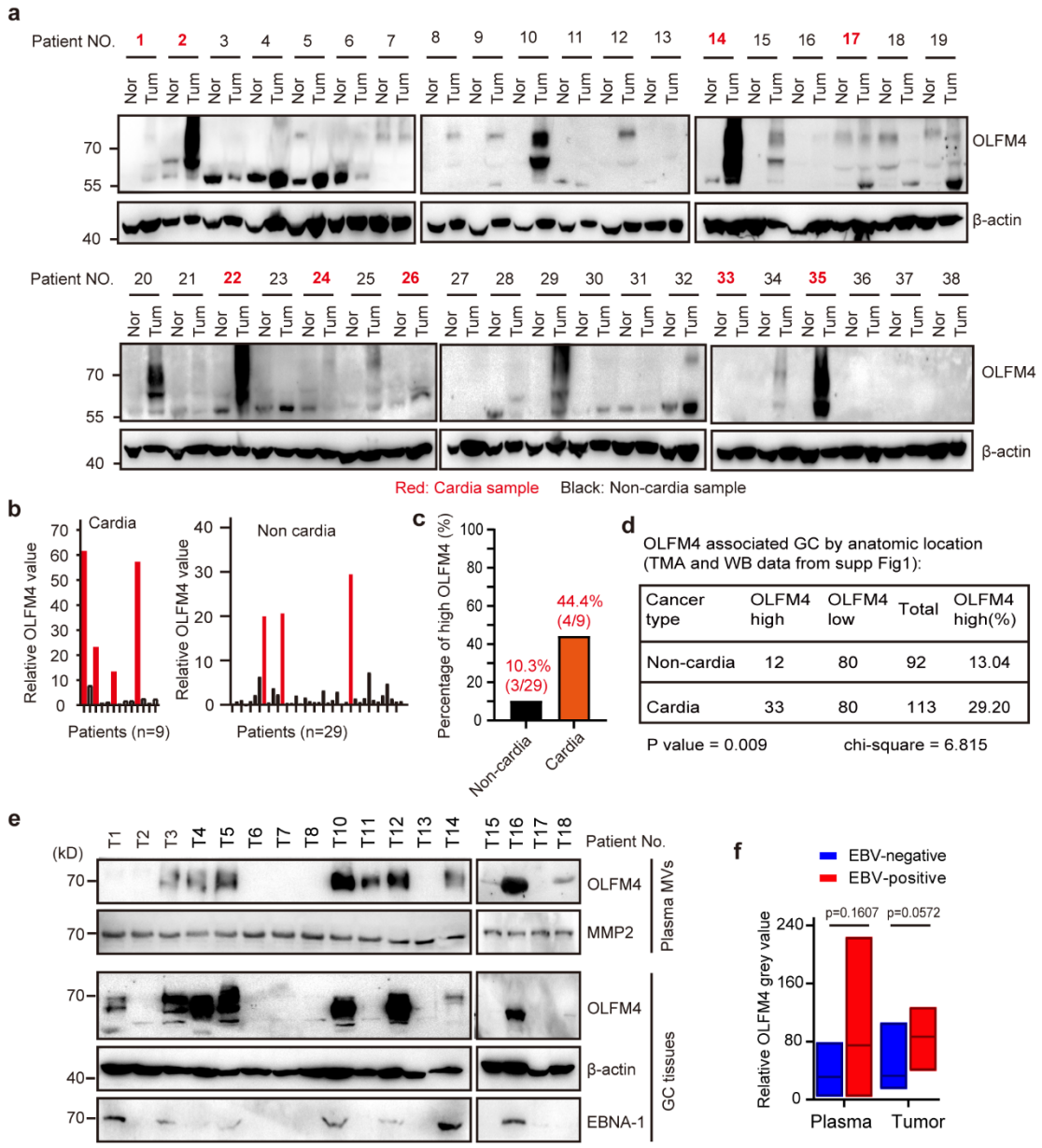

Supplementary Fig. 4 Cardiac GC is predisposed for high expression of OLFM4. a Immunoblotting showing the expression of OLFM4 in cardiac or non-cardiac gastric cancer. All lanes were loaded with 50 μg of total protein. **b** Quantification for the expression of OLFM4 protein using grey value in cardia and non-cardia samples. **c** Percentage of high OLFM4 expression (>10 fold) in cardiac and non-cardiac gastric cancer. **d** Chi-Square's test showing the correlation between anatomic location and OLFM4 expression. All immunoblotting (a) and TMA data are calculated together. **e** Immunoblotting showing the expression of OLFM4 in GC tissue and plasma MVs. All the 17 patients are cardiac GC. Total proteins and MVs were extracted from the 17 GC tissues for western blotting analysis.

For GC tissue, each lane was loaded with 50 μg of total protein. For plasma MVs, each lane was loaded with 2×10^8 MV particles. **f** Relative gray values showing the protein levels of OLFM4 in the purified MVs from the indicated samples. The center line corresponds to the median and box corresponds to the interquartile range. Data are analyzed for significant differences by performing two-tailed, one-way ANOVA with Dunnett's post hoc analysis. Source data are provided as a Source Data file.

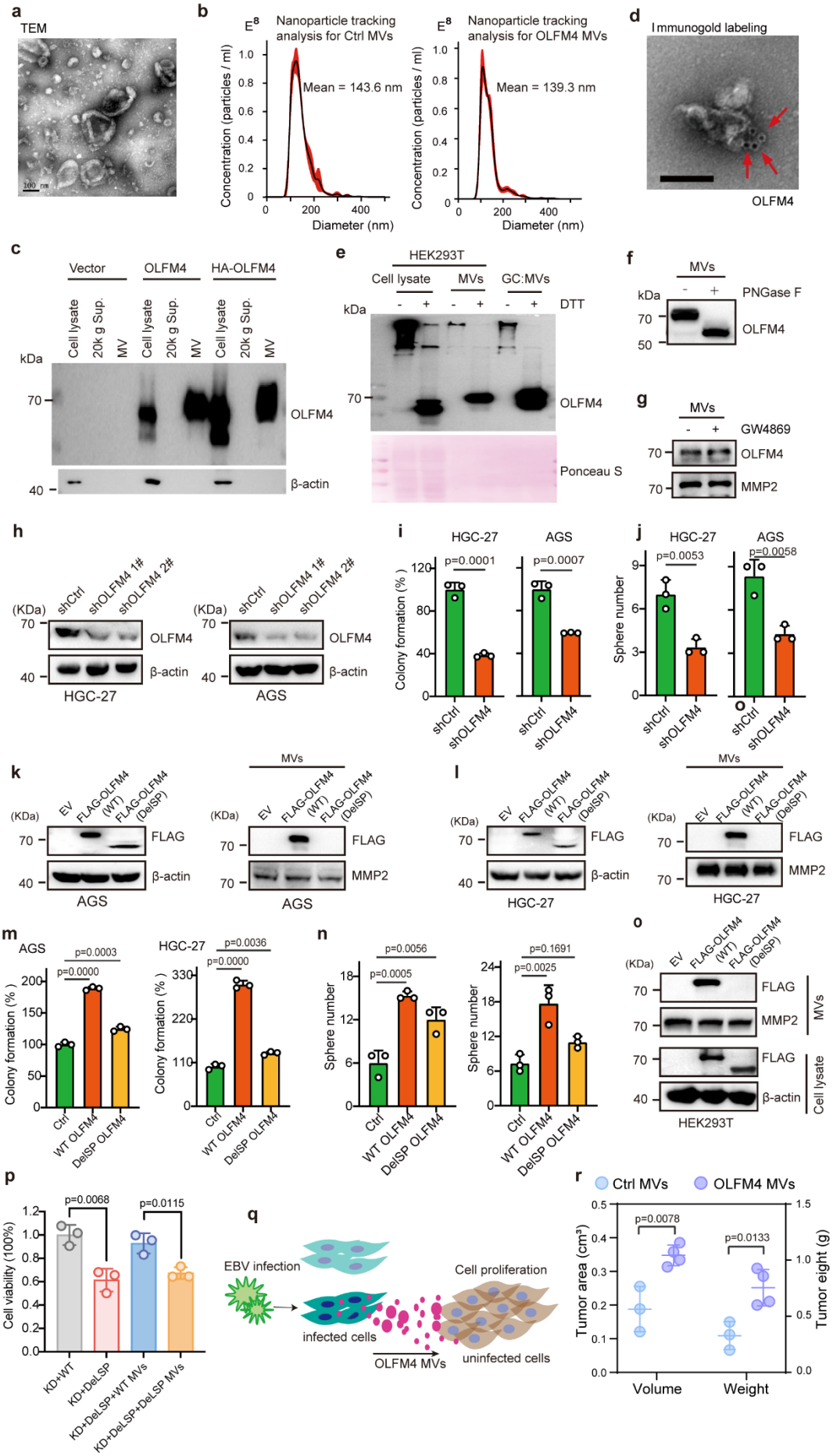
a
TEM
100 nm
b
Nanoparticle tracking analysis for Ctrl MVs
Mean = 143.6 nm
Concentration (particles / ml)
Diameter (nm)
Nanoparticle tracking analysis for OLFM4 MVs
Mean = 139.3 nm
d
Immunogold labeling
OLFM4
c
Vector
OLFM4
HA-OLFM4
Cell lysate
20k g Sup.
MV
kDa
70
40
OLFM4
β-actin
e
HEK293T
Cell lysate
MVs
GC:MVs
DTT
Ponceau S
f
PNGase F
g
GW4869
MMP2
h
shCtrl
shOLFM4 1#
shOLFM4 2#
HGC-27
AGS
i
p=0.0001
p=0.0007
Colony formation (%)
j
p=0.0053
p=0.0058
Sphere number
k
EV
FLAG-OLFM4 (WT)
FLAG-OLFM4 (DelSP)
FLAG
l
m
p=0.0003
p=0.0000
p=0.0036
n
p=0.0056
p=0.0005
p=0.1691
p=0.0025
Ctrl
WT OLFM4
DelSP OLFM4
o
p
p=0.0068
p=0.0115
Cell viability (100%)
KD+WT
KD+DelSP
KD+DelSP+WT MVs
KD+DelSP+DeLSP MVs
q
EBV infection
infected cells
OLFM4 MVs
Cell proliferation
uninfected cells
r
Ctrl MVs
OLFM4 MVs
p=0.0078
p=0.0133
Tumor area (cm³)
Tumor eight (g)
Volume
Weight

Supplementary Fig. 5 OLFM4-containing MVs promote GC cell proliferation. a Transmission electron microscopy (TEM) image of HEK293FT-derived MVs. Scale bar represents 100 nm. **b** Nanoparticle tracking analysis of ctrl- and OLFM4-MVs from HEK293T. **c** Immunoblotting showing the expression efficiency and secretion of OLFM4 in HEK293T cells transfected with empty vector, OLFM4 or HA-OLFM4. **d** Representative TEM image of immunogold-labelled OLFM4 in HEK293T derived MVs. Arrowheads indicate 10-nm gold particles. Scale bar, 100 nm. **e** Immunoblotting showing the MV-delivered OLFM4 forms disulfide-bonded multimers. **f** Immunoblotting showing the expression of OLFM4 in MVs after pretreated with 1 U PNGase F at 37°C for 12 h. **g** Immunoblotting showing the expression of OLFM4 in MVs from GW4869-treated HEK293T cells. **h** Immunoblotting showing the the knockdown efficiency of OLFM4 in HGC-27 and AGS cells. **i** Colony formation of OLFM4 knockdown HGC-27 or AGS cells (n=3 biological replicates/group). **j**. Sphere formation of OLFM4 knockdown HGC-27 and AGS cells. **k** Immunoblotting showing expression of wildtype and mutant OLFM4 (DelSP) in AGS cells and its MVs. DelSP, deletion of the signal peptide (1-20 aa) of OLFM4. **l** Immunoblotting showing expression of wildtype and mutant OLFM4 (DelSP) in HGC-27 cells and its MVs. **m** Colony formation of AGS and HGC-27 cells after transfection with wildtype OLFM4 or the DelSP mutant (n=3 biological replicates/group). **n** Sphere formation of AGS and HGC-27 cells after transfection with wildtype OLFM4 or the DelSP mutant (3 biological repeats/group). **o** Immunoblotting showing the expression of the indicated plasmid in OLFM4-knockdown HGC-27 cells. **p** Cell viability of HGC-27 cells after treatment withHEK293T-delivered MVs (3×10^8 particles/ml, n=3 biological replicates/group). **q** A working model showing that EBV-infected GC cells secrete OLFM4 MVs to stimulate overgrowth of the neighboring cells that are not infected by EBV. **r** Subcutaneous tumor formation of HGC-27 with intravenous control MVs (n=3 mice) or OLFM4 MVs (n=4 mice). All mice were euthanized 21 days after cell inoculation. Representative of 2 independent experiments (c-p,r). All data are presented as mean ± s.d., analyzed for significant differences by performing two-tailed, unpaired Student's t-tests (l,j) or one-way ANOVA with Dunnett's post hoc analysis (m,n,p,r). Source data are provided as a Source Data file.

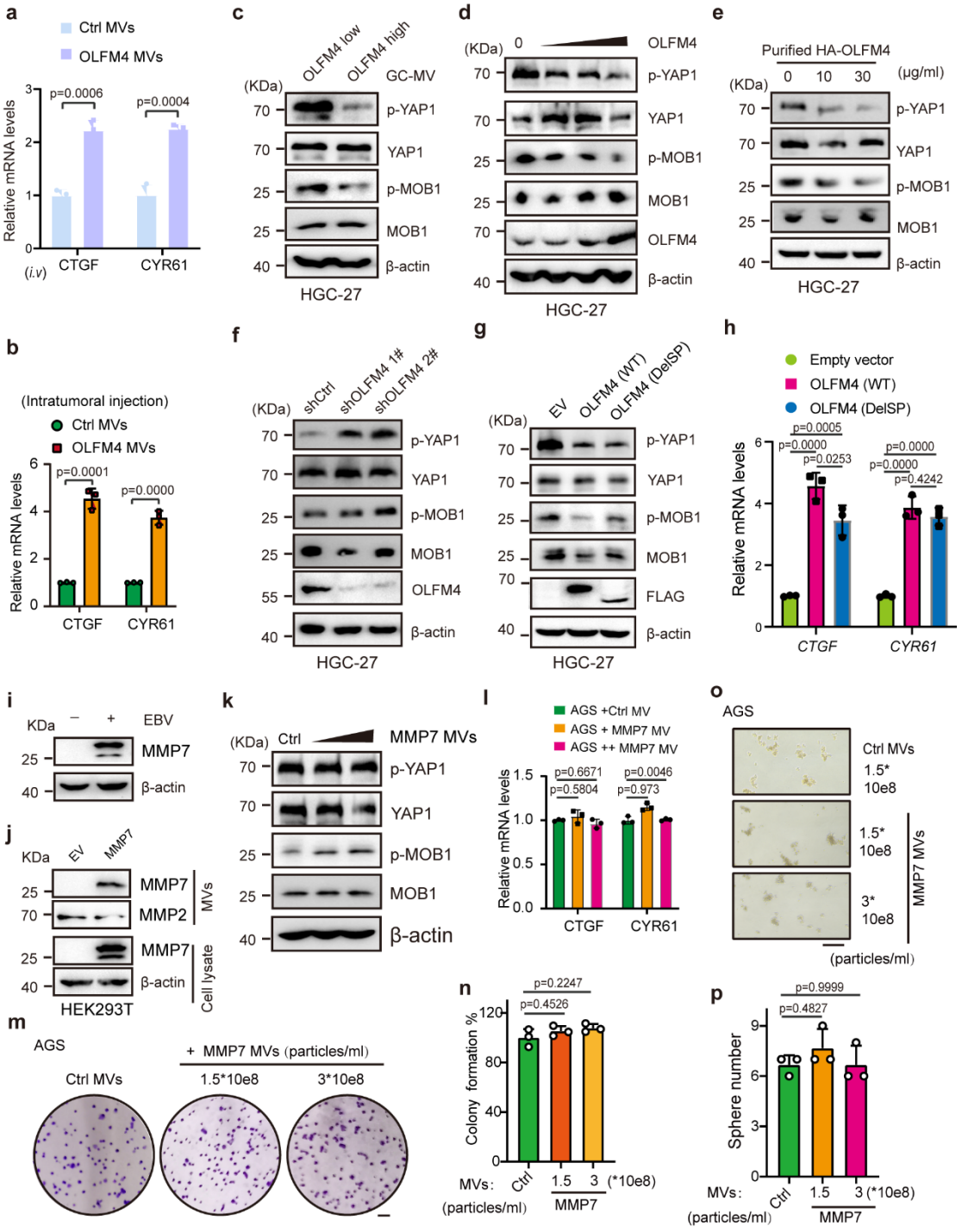

Supplementary Fig. 6 OLFM4-carried MVs promote YAP signaling and gastric tumor progress. a mRNA levels of YAP target genes in subcutaneous tumors of OLFM4 MVs intravenous injected mice. **b** mRNA levels of YAP target genes in OLFM4-overexpressing MVs-treated subcutaneous tumors (n=3 biological replicates/group). **c** Immunoblotting showing the expression of p-MOB1, MOB1, p-YAP1 and YAP1 in HGC-27 cells after treatment with high- or low- OLFM4 MVs. **d** Immunoblotting showing the expression of the

indicated proteins in HGC-27 cells after transfection with 0, 2, 4, 8 μg pcDNA3.1-OLFM4 plasmids. **e** Immunoblotting showing the expression of the indicated proteins in HGC-27 cells after treatment with purified OLFM4 proteins. OLFM4 is purified by HA beads. **f** Immunoblotting showing the expression of the indicated proteins in OLFM4-knockdown HGC-27 cells. **g** Immunoblotting of the indicated proteins in HGC-27 cells transfected with empty vector (ctrl), wild-type OLFM4 or its signal peptide deletion mutant. **h** QPCR analysis of YAP target genes (CTGF and CYR61) in the OLFM4 (DelSP)-expressing HGC-27 cells (n=3 biological replicates/group). **i** Immunoblotting showing the protein levels of MMP7 in GES-1 cells infected with 10 MOI EBV. **j** Immunoblotting showing the protein levels of MMP7 in MVs isolated from HEK293T. **k** Immunoblotting showing the levels of p-YAP1, YAP1, p-Mob1 and Mob1 in AGS cells after treatment with MMP7-overexpressing MVs (1.5, 3×10^8 particles /ml) derived from HEK293T. **l** mRNA levels of YAP target genes in MMP7 MV- treated AGS cells (n=3 biological replicates/group). **m** Representative images showing colony formation ability of MMP7 MV-treated AGS cells. Scale bars, 1.5 mm. **n** Quantification for colony formation ability in MMP7 MV-treated AGS cells (n=3 biological replicates/group). **o** Sphere formation ability of MMP7 MV-treated AGS cells. Scale bars, 200 μm. **p** Quantification for sphere formation ability in MMP7 MV-treated AGS cells (n=3 biological replicates/group). Representative of 2 independent experiments (a-p). Data are presented as mean ± s.d., analyzed for significant differences by performing two-tailed one-way ANOVA with Dunnett's post hoc analysis (a,b,h,l,n,p). Source data are provided as a Source Data file.

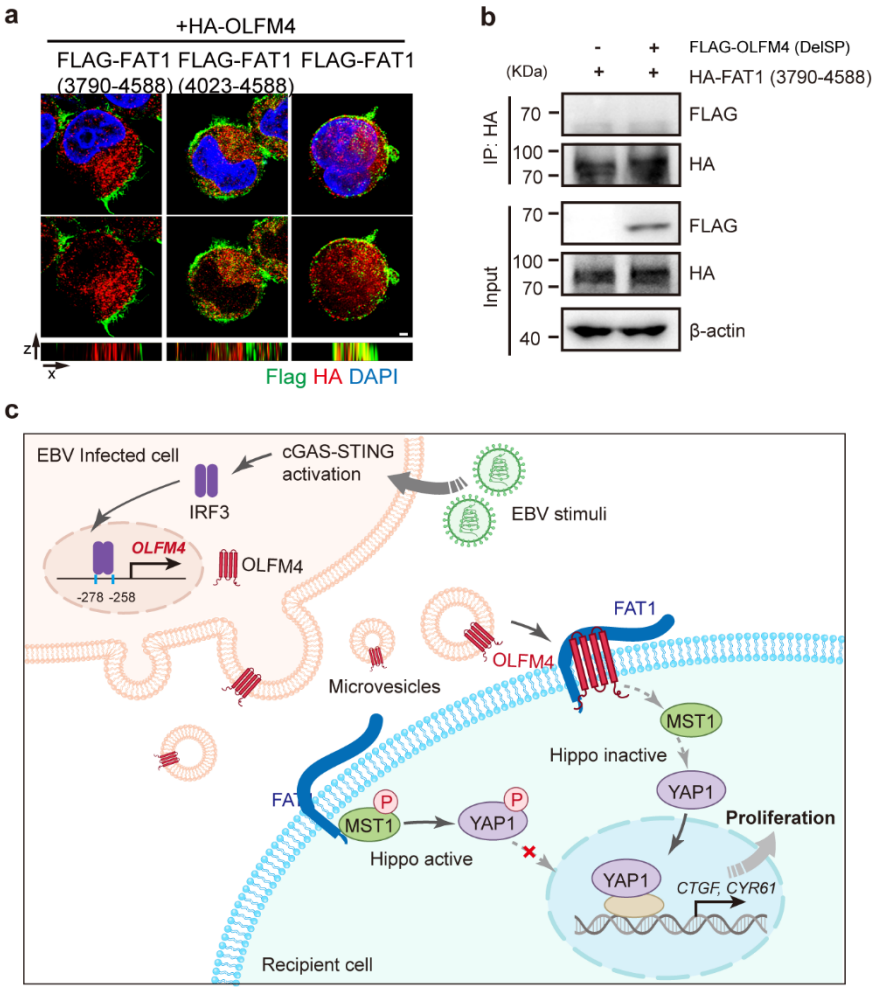

Supplementary Fig. 7 OLFM4 interacts with the extracellular region of FAT1 to inhibit Hippo signaling. a Immunofluorescent assay showing the colocalization of HA-OLFM4 and FLAG-FAT1 and its truncations. Upper, construction of FLAG tagged FAT1 with cadherins #28-33. Lower, immunofluorescent images. **b** Co-IP assay showing the interaction of HA-FAT1(3790-4588) with FLAG-OLFM4 (DelSP). **c** Scheme illustration. OLFM4 was induced by cGAS-STING pathway when cells infected with EBV, then OLFM4 was secreted via microvesicles, the OLFM4 carried by MVs binds to the FAT1 extracellular cadherin domain of recipient cells to prevent the interaction between FAT1 and Hippo kinase MST1, so as to inhibit Hippo pathway and promote cancer progression. Representative of 2 independent experiments (a,b).Source data are provided as a Source Data file.